Experimental and Computational Study of β-H Transfer between Cobalt(I) Alkyl Complexes and 1-Alkenes

Kilian P. Tellmann, Martin J. Humphries, Henry S. Rzepa,* and Vernon C. Gibson*

Department of Chemistry, Imperial College London, Exhibition Road, London SW7 2AZ, U.K.

Received June 8, 2004

Bis(imino)pyridine cobalt(I) alkyl complexes react with 1-alkenes by β-hydrogen transfer, providing a model reaction for the study of a commonly encountered chain transfer process in polymerization and oligomerization catalysis. The influence of steric effects on reaction rates is described. The theoretical models largely agree with the experimentally determined structures, provide a more detailed view of the species involved, and are consistent with the observed reactivities. Both experiment and theory support a stepwise pathway involving a cobalt-hydride intermediate.

Introduction

Some of the most highly active ethene polymerization catalysts to have been reported in recent years are based on the bis(imino)pyridine (L) ligand framework, particularly when attached to metals such as Fe and Co,[1] V,[2] and Cr.[3] The considerable difficulty of synthesising iron alkyl derivatives, the surprising inertness of second-row congeners (Ru, Rh),[4] and the paramagnetism accompanying the V and Cr systems[2,3] have made detailed study of the reactivity of long-chain metal alkyls in LMR_n species problematic.

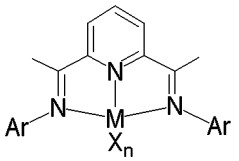

M = Fe; n = 2, 3
Co; n = 1, 2
V; n = 3
Cr; n = 3

As reported previously, it is, however, possible to isolate neutral[5,6] and ionic[5a,b] diamagnetic derivatives of bis(imino)pyridine cobalt complexes. Only the latter act as initiators for ethene polymerization, whereas the former are totally inert toward ethene if the metal-attached alkyl lacks β-hydrogens. Following successful preparation of longer chain bis(imino)pyridine cobalt(I) *n*-alkyls, we reported our initial findings on the reactivity of these complexes with alkenes.[6] A study on β-diketiminate iron alkyl complexes has afforded closely related results.[7] Further experimental investigations on the organocobalt complexes as well as supporting theoretical studies are the subject of this paper.

Experimental Results and Discussion

Synthesis, Properties, and Structure. The highly air- and moisture-sensitive cobalt(I) *n*-alkyls **I**−**VII** were prepared by reaction of divalent precursors with a slight excess of the appropriate Grignard reagent (R = Et, ^{n}Pr, ^{n}Bu, ^{n}Hx, CH_2CH_2Ph, or "PhEt") in diethyl ether to afford the desired products in good yield (Scheme 1).

These compounds are assumed to adopt a square-planar coordination geometry on the basis of their diamagnetism (16VE, d^8 configuration), the crystal structures of stable analogues $LCoCl$[5a,b] and $LCoCH_2SiMe_3$,[5c] and their apparent C_{2v} symmetry in solution (NMR). The NOE data provided in the Supporting Information is entirely consistent with this description. Attempts to synthesize cobalt(I) *n*-alkyl derivatives containing aryl substituents carrying only one *ortho*-substituent, or those bearing a branch in the α- or β-positions of the alkyl chain, were unsuccessful.

Noteworthy features of the complexes are distinctive nuclear magnetic resonances attributable to the ketimine methyl groups[8] (−1.33 to −1.35 ppm **I**−**IV**, −1.22 ppm **V**, −1.47 ppm **VI**, −1.53 ppm **VII**), the *para*-H of the pyridine ring (+10.25 ppm to +10.18 ppm **I**−**VII**), and the β-hydrogens of the alkyl chain (−1.18 ppm **I**, −0.73 ppm **II**, −0.85 ppm **III**, −0.83 ppm **IV**, +0.32 ppm **V**, −1.35 ppm **VI**, −1.16 ppm **VII**). On the basis of the following observations it was concluded that the high-

(1) (a) Britovsek, G. J. P.; Gibson, V. C.; Kimberley, B. S.; Solan, G. A.; White, A. J. P.; Williams, D. J. *Chem. Commun.* **1998**, 849. (b) Small, B. L.; Brookhart M.; Bennett, A. M. A. *J. Am. Chem. Soc.* **1998**, *120*, 4049. (c) Britovsek, G. J. P.; Bruce, M.; Gibson, V. C.; Kimberley, B. S.; Maddox, P. J.; Mastroianni, S.; McTavish, S. J.; Redshaw, C.; Solan, G. A.; Strömberg, S.; White, A. J. P.; Williams, D. J. *J. Am. Chem. Soc.* **1999**, *121*, 8728.

(2) Reardon, D.; Conan, F.; Gambarotta, S.; Yap, G.; Yang, Q. Y. *J. Am. Chem. Soc.* **1999**, *121*, 9318.

(3) Esteruelas, M. A.; López, A. M.; Méndez, L.; Oliván, M.; Oñate, E. *Organometallics* **2003**, *22*, 395. Small, B. L.; Carney, M. J.; Holman, D. H.; O'Rourke, C. E.; Halfen, J. A.; *Macromolecules* **2004**, *37*, 4375−4386.

(4) Dias, E. L.; Brookhart, M.; White, P. S. *Organometallics* **1999**, *19*, 4995.

(5) (a) Humphries, M. J.; Clentsmith, G. K. B.; Gibson, V. C.; Tellmann, K. P. *Abstracts of Papers, 222nd ACS National Meeting, Chicago, IL,* August 26−30, 2001. (b) Gibson, V. C.; Humphries, M. J.; Tellmann, K. P.; Wass, D. F.; White, A. J. P.; Williams, D. J. *Chem. Commun.* **2001**, 2252. (c) Kooistra, T. M.; Knijnenburg, Q.; Smits, J. M. M.; Horton, A. D.; Budzelaar, P. H. M.; Gal, A. W. *Angew. Chem., Int. Ed.* **2001**, *40*, 4719.

(6) (a) Tellmann, K. P.; Humphries, M. J.; Gibson, V. C. *Abstracts of Papers, 224th ACS National Meeting, Boston, MA,* August 18−22, 2002. (b) Gibson, V. C.; Tellmann, K. P.; Humphries, M. J.; Wass, D. F. *Chem. Commun.* **2002**, 2316.

(7) Vela, J.; Smith, J. M.; Lachicotte, R. J.; Holland, P. L. *Chem. Commun.* **2002**, 2886.

(8) Similar high-field chemical shifts have also been observed in diamagnetic α-diimine complexes of nickel. (a) Svodoba, M.; tom Dieck, H. *J. Organomet. Chem.* **1980**, *191*, 321. (b) tom Dieck, H.; Svodoba, M.; Greiser, T. *Z. Naturforschung.* **1981**, *36b*, 823.

10.1021/om049581h CCC: $27.50
Publication on Web 10/08/2004

Scheme 1. Synthesis of Bis(imino)pyridine Cobalt(I) *n*-Alkyl Complexes

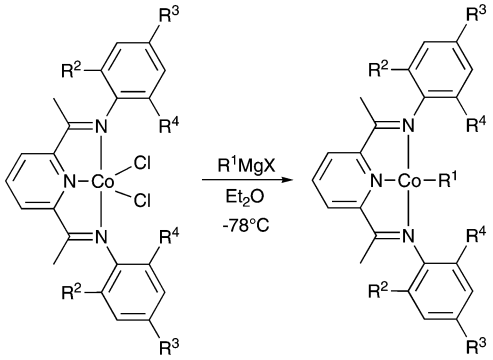

	R^1	R^2	R^3	R^4
I	Et	^{i}Pr	H	^{i}Pr
II	^{n}Pr			
III	^{n}Bu			
IV	^{n}Hx			
V	PhEt			
VI	Et	Me	Me	Me
VII	^{n}Bu			

field shifts for the latter hydrogen nuclei are not caused by β-agostic interactions:[9] (a) the one-bond $^1H-^{13}C$ coupling constants for **I** and **II** are in the range expected for non-agostic alkyl groups (123−125 Hz), and there is no pronounced change in the size of the coupling constant on moving from a β-CH_3 (**I**) to a β-CH_2 (**II**) group; (b) no appreciable change occurred in the chemical shift of the β-hydrogens in **III** on cooling a sample in d_8-toluene to 193 K nor on addition of a donor molecule such as THF or diethyl ether, which usually leads to displacement of agostic interactions. For these reasons, and in view of the approximately orthogonal orientation of the aryl ring systems to the chelate plane usually encountered in these complexes, the high-field resonances of the β-hydrogens are attributed to ring current effects.[10] The origin of the distinctive chemical shifts for the ketimine methyl and pyridyl hydrogens is less clear, although it has recently been suggested that interpretation of the molecular ground states as low-spin Co(II) antiferromagnetically coupled to a ligand radical anion, in combination with low-lying exited triplet states, may provide an explanation.[11]

Organocobalt complexes **I**−**VII** are not stable indefinitely. However, their decomposition is sufficiently slow to allow their isolation and manipulation for a few hours at room temperature. Storage in the presence of either an ethereal donor or an 1-alkene of carbon number identical to the alkyl chain suppresses the rate of decomposition markedly, but not altogether. As mentioned above, no change is observed in the NMR spectra of the cobalt(I) alkyls **I**−**VII** on exposure to ethereal donors. This is also the case for 1-alkene partners of identical carbon number, with each compound appearing unperturbed by the presence of the other, even by the methods of polarization transfer (NOE, EXSY). Despite this, isotopic scrambling is observed between LCoEt (**I**) and C_2D_4 suggesting that, while exchange is slow on the NMR time scale, it is frequent enough to significantly inhibit decomposition. Lower temperatures also have a beneficial impact on the lifetime of complexes **I**−**VII**. On decomposition, several diamagnetic products are formed, the only unambiguously identified byproduct being the alkane R−H (ethane, propane, and butane for **I**−**III**, respectively). The other, unidentified decomposition products appear as complexes of lower symmetry than the starting material. Presumably, irreversible elimination of the hydrocarbon moiety R−H from the organocobalt complexes occurs concomitant to, or as a consequence of, ligand C−H activation.

Scheme 2. Reaction of Cobalt(I) *n*-Alkyl Complexes with Ethene via *β*-H Transfer

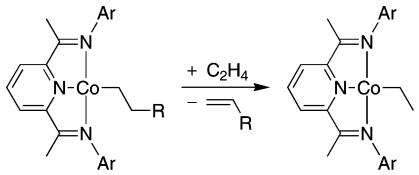

Table 1. Selected Kinetic Data for *β*-H Transfer from Complexes II−V and VII to Ethene

starting material	T (K)	reaction half-life ($t_{1/2}$) (min)	relative reaction rates vs **VII** (at 294 K)	relative reaction rates vs **V** (at 300 K)
II	294	40.0	3.64	
III	294	179.2	16.3	
III	300	92.5		6.01
IV	300	66.1		4.29
V	294	68.3	6.21	
V	300	15.4		1.00
VII	294	11.0	1.00	

Kinetics and Mechanism of *β*-H Transfer. Exposure of **II**−**V** or **VII** to ethene leads to formation of **I** or **VI** and CH_2=CHR (R = H, Me, Et, ^{n}Bu, Ph), thus offering the opportunity to gain insight into the steric and electronic influences of bis(imino)pyridine ligands on the reactivity of their associated metal alkyls.

The conversion of the longer chain cobalt-alkyl species **II**−**V** and **VII** to the cobalt ethyl complexes **I** and **VI** (Scheme 2) may be conveniently followed by NMR spectroscopy, revealing a first-order dependence of the reaction rate on [$LCoCH_2CH_2R$] and a zero-order dependence on [ethene] in each case. The summary of the kinetic data provided in Table 1 gives an indication of the effects influencing the overall reaction rate, chiefly the length of the n-alkyl chain and the steric constraints of the ligand. For instance at 294 K, β-H transfer for the n-propyl derivative **II** proceeds 4.48 times faster than for the n-butyl derivative **III**, due, it is presumed, to increased steric congestion in the transition state for the n-butyl species. Similarly, the reaction of the 2-phenylethyl derivative **V** with ethene proceeds substantially

(9) Brookhart, M.; Green, M. L. H.; Wong, L.-L. *Progr. Inorg. Chem.* **1988**, *36*, 1.

(10) The "quasi-aromatic nature" of transition metal containing chelate rings may provide a rationalization for some of the observed effects. The properties of five-membered, 2,4-unsaturated metal-containing rings have been described by: Bayer, E. *Angew. Chem.* **1964**, *76*, 76.

(11) Knijnenburg, Q.; Hetterscheid, D.; Kooistra, T. M.; Budzelaar, P. H. M. *Eur. J. Inorg. Chem.* **2004**, 1204.

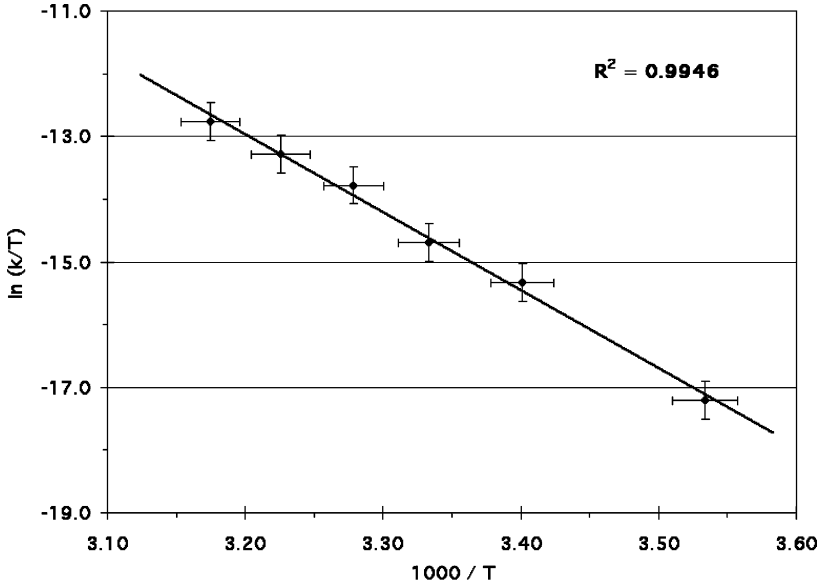

Figure 1. Eyring plot for the reaction of LCo^{n}Bu **III** with ethene in C_6D_6.

faster at 300 K than for either complex **III** or **IV**, but slower than for **II**. Furthermore, the rate of β-H transfer to ethene takes place faster in complexes with smaller *ortho*-substituents in the bis(imino)pyridine ligand: Reaction of the *n*-butyl complex **VII** (Ar = 2,4,6-$Me_3C_6H_2$) with ethene proceeds 16.3 times faster than for derivative **III** (Ar = 2,6-$^i Pr_2C_6H_3$), indicative of a significantly lower barrier in the transition state ($\Delta\Delta G^{\ddagger} = \Delta G^{\ddagger}_{\mathbf{VII}\rightarrow\mathbf{I}} - \Delta G^{\ddagger}_{\mathbf{III}\rightarrow\mathbf{I}} = 1.63$ kcal mol^{-1}).

In addition to this, C−H bond-breaking was inferred in the transition state of the rate-determining step in view of a kinetic isotope effect (KIE) of 3.32 (0.04) for the conversion of d_9-**III** into d_5-**I** by d_4-ethene at 300 K. The alkyl chain and the 1-alkene had to be fully deuterated in order to avoid complications arising from H/D scrambling. The magnitude of the observed KIE is about half that of the usually anticipated primary KIE for C−H bonds (but much larger than a secondary KIE), in accordance with expected deviations arising from nonlinear movement through the transition state,[12] as would be anticipated for this type of hydrogen transfer.

To obtain further insight into the nature of the transition state, the reaction of **III** with ethene was also followed over the temperature range 283−315 K. With clean transformations occurring in each case, an Eyring plot (Figure 1) was obtained and the activation parameters were determined as $\Delta H^{\ddagger} = 24.7 \pm 0.9$ kcal mol^{-1} and $\Delta S^{\ddagger} = 6 \pm 3$ cal mol^{-1} K^{-1} ($\Delta G^{\ddagger}_{298} = 22.9 \pm 0.9$ kcal mol^{-1}). The two most plausible reaction profiles as limiting cases for β-H transfer are shown in Scheme 3: Path A proceeds via a stepwise, dissociative mechanism with four-centered transition states, whereas path B follows a concerted, associative mechanism having a six-centered transition state. The relatively small entropy of activation along with the independence of the reaction rate on ethene pressure is more consistent with path A, since the involvement of ethene in the transition state for path B would be anticipated to afford a first-order dependence on [C_2H_4] and a strongly negative entropy of activation.

The postulated reaction intermediate of path A is LCoH **VIII**. This compound is generally accessible by the reaction of a cobalt(I) alkyl (LCoMe,[5] LCoEt **I**, LCo^{n}Bu **III**) with dihydrogen in situ and, while we were unable to locate the hydride resonance by NMR (I_{Co} = 7/2), a strong absorption in the IR spectrum at 2092 cm^{-1} was attributed to the Co−H stretch. Furthermore, the description of **VIII** as LCoH is supported by the observation of either methane, ethane, or butane as the reaction by-product, depending on the alkyl precursor employed. Isolation of **VIII** has not proven possible because of the compound's pronounced sensitivity and instability toward elimination of free ligand. No further stability is imparted by isotopic substitution to give LCoD due to scrambling of the isotopic label into the *ortho*-^{i}Pr groups of the ligand to afford (*d*-L)CoH, as demonstrated by the ^{1}H and ^{13}C NMR data of complex d_n-**VIII**, as well as the mass spectra of the free ligand recovered after hydrolysis of the complex.

Scheme 3. Plausible Mechanistic Pathways for β-Hydrogen Transfer[a]

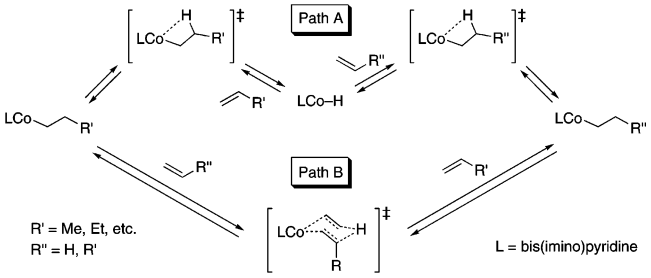

[a] Path A is favored on the basis of experimental observations.

The reaction of **VIII** with 1-alkenes (e.g., ethene, propene, 1-butene) yields the anticipated cobalt(I) *n*-alkyls **I**−**III**, lending further weight to the description of **VIII** as LCoH (Scheme 4). The alkene insertion into the cobalt−hydride bond is very rapid at room temperature (≪5 min) and therefore does not allow for a determination of the relative rates of alkene insertion. Crucially, though, this insertion is much faster than the typical rates of β-H transfer, providing additional support for the mechanism to proceed in stepwise fashion

(12) More O'Ferrall, R. A. *J. Chem. Soc. (B)* **1970**, 785.

Scheme 4. Preparation of the Cobalt-Hydride Complex VIII and Its Reactivity toward 1-Alkenes

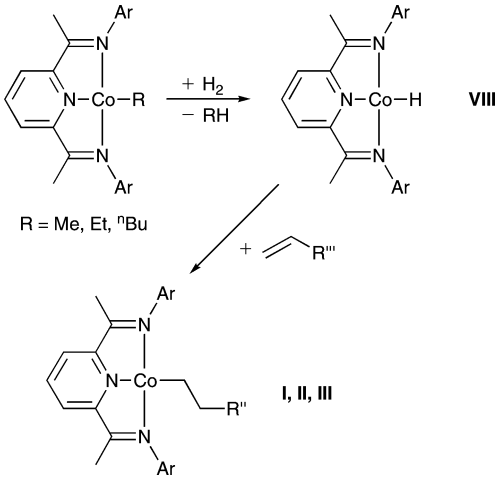

(path A), rate-limited by elimination of alkene to the high-energy intermediate **VIII**.

When using higher 1-alkenes instead of ethene in the alkene exchange reaction, an equilibrium not far from unity is attained. From a kinetic perspective, for instance, the initial rate of reaction between LCo^{n}Bu **III** and propene (to give **II** and 1-butene) is virtually identical to that of β-H transfer from **III** to ethene up to 95% of the first half-life. If the concerted path B were followed, it would be expected that incorporation of propene into the transition state would lead to a significant increase in steric congestion and thereby reduce the rate of the reaction, whereas the transition state for path A does not involve the incoming monomer. Also, the equilibrium between **II** and **III** is reached by reversible first-order kinetics (first order in either LCoR species). Given the similarity of propene and 1-butene, in combination with the extra steric requirements of the additional substituent on the alkene in an associative transition state, a change from first-order to second-order kinetics might be anticipated if path B were the predominating mechanism. The equilibrium however is attained by reversible first-order kinetics, which is fully consistent with observations made for β-H transfer to ethene and the stepwise reaction path A in Scheme 3.

Thermodynamic Aspects. As alluded to above, alkyl exchange via β-H transfer between the longer chain cobalt n-alkyl complexes and higher 1-alkenes ($\geq C_3$) occurs readily, as well as reversibly, at stoichiometric concentrations, with K_{eq} near unity. This was exemplified for equilibria between complexes **II/III**, **II/IV**, and **III/IV** in combination with the appropriate 1-alkene pairs and is hence assumed to be general for LCoR complexes.

Indeed, a reversal of the alkyl exchange reactions that afford thermodynamically more stable LCoEt **I** is possible when using large excesses of a 1-alkene (Scheme 5): Addition of excess 1-hexene to a solution of LCoEt **I** in d_6-benzene leads to the formation of detectable quantities of the targeted cobalt n-alkyl **IV** together with an equimolar quantity of ethene.

Unfortunately, however, an accurate determination of the equilibrium constants for β-H transfer between the higher cobalt n-alkyls is severely complicated by a side reaction, in which the 1-alkenes present in the

Scheme 5. Reversible Displacement of 1-Alkenes from LCoR Complexes

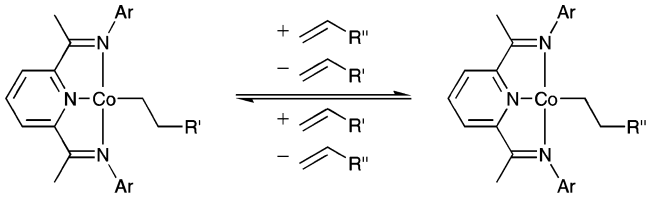

mixture are isomerized to internal alkenes at rates not markedly slower than those of the exchange reactions. Since internal alkenes do not appear to participate in β-H transfer (consistent with failure to isolate α- or β-branched cobalt(I) alkyls), the equilibrium is observed to drift over time. For this reason some uncertainty remains over the extent of adaption of the ratio of cobalt n-alkyls to the varying concentration of 1-alkenes at any stage and, hence, the accuracy of the calculated values of K_{eq}. In general, though, it can be stated that the longer-chain cobalt n-alkyl complexes **II**–**IV** are all very similar in energy from a thermodynamic perspective (ΔG ca. 1 kcal mol^{-1}), but higher in energy than the cobalt ethyl **I** by around 3.5–4.0 kcal mol^{-1} at room temperature.

Consideration of the isodesmic equation

$$\text{ethene} + n\text{-butane} = \text{ethane} + \text{1-butene}$$

illustrates that the thermodynamic stability of a substituted alkene (such as 1-butene) is greater than that of an unsubstituted alkene (such as ethene) by 3.2 kcal mol^{-1} at 298 K.[13] Evidently, the exothermicity of alkyl exchange reactions that afford LCoEt **I** plus 1-alkene (ΔG about 3.5–4.0 kcal mol^{-1}) is predominantly accounted for by the greater stability of the alkene moiety, with a further, modest contribution due to the increased stability of the organometallic complex.

Experimental Conclusions

In summary, the experimental observations strongly indicate that β-H chain transfer proceeds via a stepwise mechanism involving a cobalt-hydride intermediate rather than a concerted process involving direct β-H transfer to monomer. However, further investigation of this reaction was warranted, particularly in view of the apparent differences between the reactivity of the cobalt(I) n-alkyls **I**–**VII** and the highly active bis(imino)-pyridine cobalt polymerization system. In the catalytically active system chain termination by β-H transfer is first order in ethene concentration (based on the observation that PE molecular weight is independent of ethylene pressure), implying involvement of an ethene molecule in the process. Also, the reactivity described in this article represents a chain *shortening* process, in stark contrast to the highly efficient chain *growth* process of the polymerization system.

We thus decided to explore the computed potential energy surface for the compounds central to the mech-

(13) Robert C. Weast, Ed.-in-chief. *Handbook of Chemistry and Physics*, 58th ed.; CRC Press: Cleveland, OH, 1977.

Scheme 6. Schematic for the Free Energy Surface for Stationary Points 1−16 (Ar = R = H)[a]

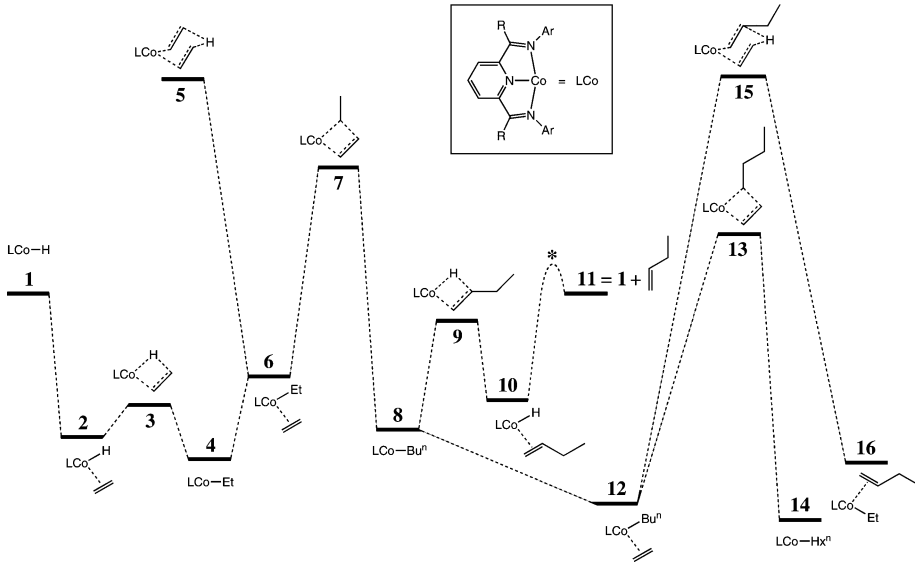

[a] Stationary points **1**−**6** relate to ethene exchange, **7**, **8**, and **12**−**14** relate to alkene polymerization, and **9**−**11** relate to alkene exchange. The existence of the point marked with the asterisk (*) is inferred on the free energy rather than potential energy surface (see main text).

anism, as well as the energies of the transition states connecting them. To differentiate unambiguously between computational results and experimentally characterized species, separate numbering schemes have been adopted for each section, using **I** (or **VI**) = **4**, **III** (or **VII**) = **8**, **IV** = **14**, and **VIII** = **1** (cf. Schemes 1, 6). The nomenclature employed in the computational section does not distinguish explicitly between the more subtle ligand substitution patterns (Ar = 2,6-$^{i}Pr_2C_6H_3$ versus Ar = 2,4,6-$Me_3C_6H_2$). As a general guideline, even arabic numerals correspond to minima in the potential surface, whereas odd arabic numerals denote transition states.

Computational Discussion

Basis Set Quality. It was thought imperative to establish the appropriate basis set level to use in exploring the overall potential surface using the B3LYP hybrid density functional procedure. The key intermediates in the overall scheme (Scheme 6) are the cobalt alkyls **4**, **8**, and **14** (and the parent hydride **1**) and the effects of ligand substitution (at Ar and R) upon these species. At an initial 6-31(d) basis set level on all atoms, including the cobalt, we noted that the hydrogen of the Co−H bond of **1** was computed to lie significantly above the plane of the ligand chelate. We felt this result might be basis set dependent, and indeed increasing the basis to 6-31G(d,p) on C, H, and N and to 6-311G(d) for Co [subsequently simply referred to as 6-31G(d,p)] planarizes this metal center. At this enlarged basis, and for Ar = R = H, the geometries of the cobalt *n*-alkyls **4** and **8** still reveal significant nonplanarity at the Co center, due to agostic interactions with a β-hydrogen of the alkyl chain. The Co···H bond lengths in **4** are 1.719/1.725 Å [6-31G(d)/6-31(d,p)]. An alternative α-agostic conformation was also located for **4**, which is higher than the β form by 0.6 kcal mol^{-1} in free energy. Further expansion of the basis set to 6-311(d,p) or 6-311(3d,p) on all atoms has an insignificant effect on the metal geometries in these various species, and we considered the 6-31G(d,p)/Co:6-311G(d) combination as suitable for further studies.

Overview of Potential Surface. The reactions shown in Scheme 6 involve both associative and dissociative pathways, with accompanying changes in entropy. To compare the energies on an equal scale, we calculated the zero-point, thermal, and entropy corrected free energies based on (unscaled) vibrational frequencies, evaluated for optimized geometries using the Gaussian programs[14] and the 6-31G(d,p)/Co:6-311G(d) basis. For Ar = R = H, the following general surface characteristics are revealed (Scheme 6). The initial reaction in this system involves coordination of ethene to **1** to form a π complex **2** (−14.5 kcal mol^{-1}), followed by insertion across the Co−H bond to create the Co−Et alkyl **4**, via a transition state **3**, exhibiting only a small barrier (1.6 kcal mol^{-1} from **2**). The overall (total energy) exothermicity from **1** + ethene to **4** is −19.0 kcal mol^{-1}. Repeating this process from **4** to **8** via **6** but with Co−H insertion replaced by Co−C insertion reveals an exothermicity of −11.2 kcal mol^{-1}, but with the barrier **7** (21.8 kcal mol^{-1} from **6**) being much higher than for Co−H insertion. A third insertion step from **8** to **14** via **12** shows little change from the second step, being exothermic by −10.8 kcal mol^{-1}.

The two alternative alkene exchange mechanisms bifurcate from the C−C bond formation (polymerization) route at structure **8**. In the first of these, **8** could instead undergo β-H abstraction by Co via transition state **9** to give **10**, followed by dissociation of butene to give **11** (=**1** + butene). These points are +5.6, +3.7, and +14.5 kcal mol^{-1} relative to **8** in free energy. The second exchange mechanism bifurcates from either **6** or its homologue **12** via the associative transition states **5** or **15**, representing concerted β-hydrogen transfer to alkene. This route has barriers of 44.8/43.2 kcal mol^{-1} from **6/12**. An equivalent, but stepwise, route for alkene exchange can also be accomplished by following the pathway **6**−**4**−**3**−**2**−**1** (overall barrier 23.4 kcal mol^{-1}) or the homologous **12**−**8**−**9**−**10**−**11** (barrier 18.9 kcal mol^{-1}).

Effect of Ligand Bulk on the Cobalt Alkyl Complexes. We next addressed the real, i.e., fully substituted, system by extending the basis set layer model to include the Ar = 2,6-$^{i}Pr_2C_6H_3$ and R = Me groups, described with the minimal STO-3G basis. To establish at least approximately the extent to which this basis adequately reproduces the steric interactions exerted by the bulky aryl groups, we compared the B3LYP/STO-3G energies for *cis*- and *trans*-1,2-dimethyl-1,2-di(*tert*-butyl)ethene,[15] for which the latter is known to have the lower enthalpy of formation by −8.6 kcal mol^{-1}. The B3LYP/STO-3G energies give a difference of −6.6 kcal mol^{-1}. This suggests that steric effects modeled this way will be only slightly underestimated.

The first task was to analyze the effect of the bulky ligands on the agostic interactions previously calculated for **4** and **8**. With Ar = 2,6-$^{i}Pr_2C_6H_3$ and R = H, the Co···H agostic length compresses from 1.744 to a shorter 1.707 Å. In contrast, for the larger *n*-butyl group in **8**, the Co···H agostic distance lengthens to 1.768 Å (Ar = 2,6-$^{i}Pr_2C_6H_3$, R = H), due to induced twisting of the agostic conformation by interaction between the terminal ethyl group of the butyl side chain and the aryl substituents. This steric compression induces a further new nonagostic conformation (Figure 2) not found with the unsubstituted systems. For **4** (Ar = 2,6-$^{i}Pr_2C_6H_3$, R = H) this is still higher than the agostic form, but for **8** (Ar = 2,6-$^{i}Pr_2C_6H_3$, R = H) it becomes lower in free energy by 0.4 kcal mol^{-1}.

Buttressing the aryl group by addition of the methyl substituent (R = Me) to the ligand amplifies these effects. In the case of **4** (Ar = 2,6-$^{i}Pr_2C_6H_3$, R = Me) the Co···H agostic length is now compressed to 1.705 Å, and chain twisting in **8** (Ar = 2,6-$^{i}Pr_2C_6H_3$, R = Me) further increases Co···H to 1.809 Å (Figure 2). The additional R = Me group completes inhibition of the agostic conformations, both LCoEt **4** and LCo^{n}Bu **8** now being predicted to prefer nonagostic conformations by 1.7 and 3.3 kcal mol^{-1} in the free energies. This is in agreement with experimental observations made for **8**, which show no significant thermal population of such conformations.

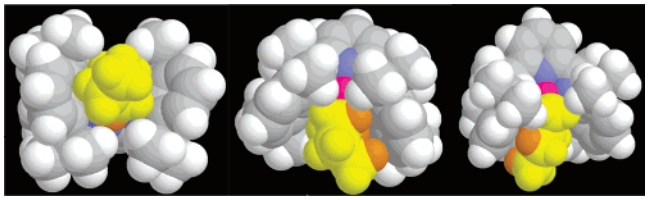

Figure 2. Space-filling representations for **8**, where Ar = 2,6-$^{i}Pr_2C_6H_3$ and R = Me, showing (a) the snug fit of the *n*-butyl group (yellow) into the coordination site on the cobalt center, accompanied by the tilting of the aryl groups for the agostic conformation; the agostic hydrogen is shown in orange; (b and c) two lower energy nonagostic conformations, for which the C−H···π bonded hydrogens are depicted in orange.

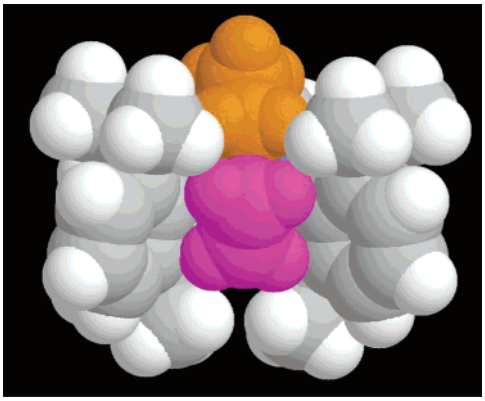

Figure 3. Space-filling representation for **6**, where Ar = 2,6-$^{i}Pr_2C_6H_3$ and R = Me, showing coordinated ethene (magenta) and Co-ethyl (orange), separated by the bulk of the isopropyl groups. The distance between the nearest two, nonbonded carbon atoms of the ethyl chain and the coordinated ethene is 2.708 Å.

The nonagostic conformation of **8** (Ar = 2,6-$^{i}Pr_2C_6H_3$, R = Me) has some further interesting features. An all-*anti* orientation of the *n*-butyl side chain allows parallel alignment with the face of one of the aryl groups, thereby maximizing the C−H···π interactions (Figure 2c); an even lower energy conformation (by 1.4 kcal mol^{-1}) adopts a *gauche* orientation in the *n*-butyl chain, again with the effect of enhancing the C−H···π bonding (Figure 2b). If the aryl substituents are changed to Ar = 2,4,6-$Me_3C_6H_2$, the greater steric bulk at the 4-position equalizes the free energies of the two C−H···π bonded conformations.

Effect of Ligand Bulk on Co-Alkene Complexes. It is evident from the preceding section that the steric bulk of the ligand has a pronounced effect on geometries, conformations, and energies of the cobalt *n*-alkyls (**4**, **8**, **14**). The effect on the cobalt complexes containing π-bonded alkenes (**2**, **6**, **12**) may be expected to be even larger because of the greater steric requirements of these in the metal coordination sphere (Figure 3). Thus ΔG for the equilibria **1**, **4**, **8** + ethene = **2**, **6**, **12** are −14.5, −4.5, and −4.4 kcal mol^{-1} for the unsubstituted ligand system of low bulk (Ar = R = H), but −14.8, +2.6, and +7.0 kcal mol^{-1} for the fully substituted ligand framework (Ar = 2,6-$^{i}Pr_2C_6H_3$, R = Me). This reveals significant steric and entropic inhibition of π complex formation, which increases with the size of the ac-

(14) (a) Frisch, M. J.; Trucks, G. W.; Schlegel, H. B.; Scuseria, G. E.; Robb, M. A.; Cheeseman, J. R.; Zakrzewski, V. G.; Montgomery, J. A., Jr.; Stratmann, R. E.; Burant, J. C.; Dapprich, S.; Millam, J. M.; Daniels, A. D.; Kudin, K. N.; Strain, M. C.; Farkas, O.; Tomasi, J.; Barone, V.; Cossi, M.; Cammi, R.; Mennucci, B.; Pomelli, C.; Adamo, C.; Clifford, S.; Ochterski, J.; Petersson, G. A.; Ayala, P. Y.; Cui, Q.; Morokuma, K.; Malick, D. K.; Rabuck, A. D.; Raghavachari, K.; Foresman, J. B.; Cioslowski, J.; Ortiz, J. V.; Stefanov, B. B.; Liu, G.; Liashenko, A.; Piskorz, P.; Komaromi, I.; Gomperts, R.; Martin, R. L.; Fox, D. J.; Keith, T.; Al-Laham, M. A.; Peng, C. Y.; Nanayakkara, A.; Gonzalez, C.; Challacombe, M.; Gill, P. M. W.; Johnson, B. G.; Chen, W.; Wong, M. W.; Andres, J. L.; Head-Gordon, M.; Replogle, E. S.; Pople, J. A. *Gaussian 98* (revision A.11); Gaussian, Inc.: Pittsburgh, PA, 1998. (b) Frisch, M. J.; Trucks, G. W.; Schlegel, H. B.; Scuseria, E.; Robb, M. A.; Cheeseman, J. R.; Montgomery, J. R., Jr.; Vreven, T.; Kudin, K. N.; Burant, J. C.; Millam, J. M.; Iyengar, S. S.; Tomasi, J.; Barone, V.; Mennucci, B.; Cossi, M.; Scalmani, G.; Rega, N.; Petersson, G. A.; Nakatsuji, H.; Hada, M.; Ehara, M.; Toyota, K.; Fukuda, R.; Hasegawa, J.; Ishida, M.; Nakajima, T.; Honda, Y.; Kitao, O.; Nakai, H.; Klene, M.; Li, X.; Knox, J. E.; Hratchian, H. P.; Cross, J. B.; Adamo, C.; Jaramillo, J.; Gomperts, R.; Stratmann, R. E.; Yazyev, O.; Austin, A. J.; Cammi, R.; Pomelli, C.; Ochterski, J. W.; Ayala, P. Y.; Morokuma, K.; Voth, G. A.; Salvador, P.; Dannenberg, J. J.; Zakrzewski, V. G.; Dapprich, S.; Daniels, A. D.; Strain, M. C.; Farkas, O.; Malick, D. K.; Rabuck, A. D.; Raghavachari, K.; Foresman, J. B.; Ortiz, J. V.; Cui, Q.; Baboul, A. G.; Clifford, S.; Cioslowski, J.; Stefanov, B. B.; Liu, G.; Liashenko, A.; Piskorz, P.; Komaromi, I.; Martin, R. L.; Fox, D. J.; Keith, T.; Al-Laham, M. A.; Peng, C. Y.; Nanayakkara, A.; Challacombe, M.; Gill, P. M. W.; Johnson, B.; Chen, W.; Wong, M. W.; Gonzalez, C.; Pople, J. A. *Gaussian 03* (revision B.04); Gaussian, Inc.: Pittsburgh, PA, 2003.

(15) Gano, J.; Lenoir, D.; Park, B.-S.; Roesner, R. A. *J. Org. Chem.* **1987**, *52*, 5636.

Scheme 7. Scheme for Alkene Exchange[a]

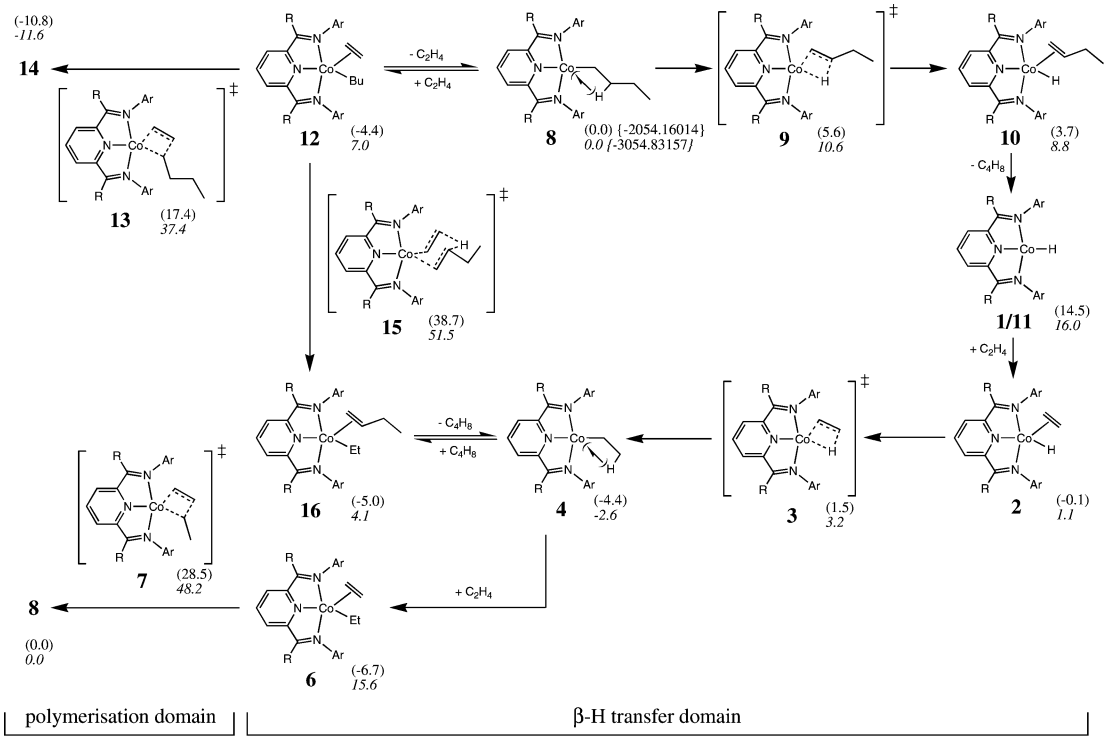

[a] Free energies (kcal mol^{-1}) for Ar = R = H (bracketed) and Ar = 2,6-^{i}Pr$_2$C$_6$H$_3$, R = Me (italics) are shown relative to **8** + ethene.

companying Co-alkyl side chain. Such inhibition of π complex formation agrees with the lack of detection of such π complexes experimentally.

Transition States. Having established the basic features of the potential surface, and the effect of steric compression upon it with the Ar and R groups, we turn to discussing in more detail the free energy barriers for both alkene exchange and alkene insertion/polymerization (Scheme 7).

Steric Effects on the Alkene Polymerization. We discuss first the reaction that is observed *not* to occur, namely, the C−C bond formation between the cobalt *n*-alkyl group and the coordinated alkene, which would ultimately result in polymerization (rather than alkene exchange by β-H transfer). The key transition states are **7** (ethyl/ethene C−C formation) and **13** (*n*-butyl/ethene C−C formation). The free energy barrier of **7** relative to **6** (Ar = R = H) is 21.8 kcal mol^{-1}, rising to 32.6 kcal mol^{-1} for the fully substituted ligand (Ar = 2,6-^{i}Pr$_2$C$_6$H$_3$, R = Me). Inspection of the geometry of **7** reveals that the least hindered orientation of the methyl group (Figure 4a) encounters steric congestion from the aryl groups, rationalizing the 10.8 kcal mol^{-1} increase in the barrier induced by increasing the ligand bulk. The ethene dimerization reaction is therefore sterically inhibited to a significant degree. Likewise, formation of the cobalt *n*-hexyl product **14** via transition state **13** from reactant **12** has free energy barriers of 21.8 (for Ar = R = H) and 37.4 kcal mol^{-1} (for Ar = 2,6-^{i}Pr$_2$C$_6$H$_3$, R = Me), again indicating little probability of reaction by this route.

Steric Effects on Alkene Exchange Mechanism. We now turn to the reaction that *is* observed. Transition point **5**, Ar = R = H, which corresponds to associative ethene exchange, has a computed free energy barrier

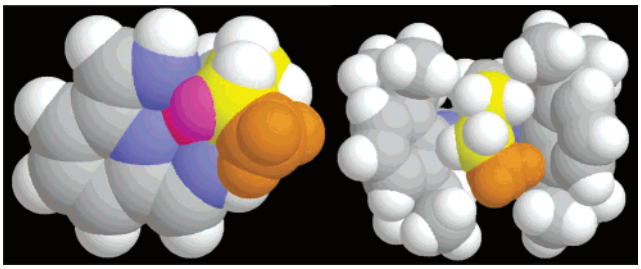

Figure 4. Space-filling representations for (a) **7** with Ar = R = H, showing C−C forming bond (yellow) and methyl (orange) substituent; the alternative *endo*-facing conformation for the methyl group (replacing the magenta hydrogen) encounters hindrance from the ligand face; and (b) **7** with Ar = 2,6-^{i}Pr$_2$C$_6$H$_3$, R = Me.

of 44.8 kcal mol^{-1} (computed relative to **6** to facilitate comparison with the C−C polymerization route). This increases to 48.8 kcal mol^{-1} with Ar = 2,6-^{i}Pr$_2$C$_6$H$_3$, R = Me (Figure 5), revealing a steric inhibition of this associative route of +4.0 kcal mol^{-1}. The analogous alkene exchange mechanism between the cobalt *n*-butyl complex and ethene involves the equilibrium between **12** and **16** connected via transition state **15**. This point has a free energy (relative now to **12**) of 43.2 kcal mol^{-1} (Ar = R = H) and 44.5 kcal mol^{-1} (Ar = 2,6-^{i}Pr$_2$C$_6$H$_3$, R = Me), this time revealing a rather smaller steric inhibition. In general, however, these all represent very high thermal barriers, making it highly unlikely that alkene exchange reactions could proceed by this route at typical (ambient) temperatures.

Seeking alternative lower energy routes for alkene exchange, we turned to the dissociative routes from **6** to **1**, or the homologous pathway from **12** to **11**. The overall free energies for the route from **6** to **1** (+2

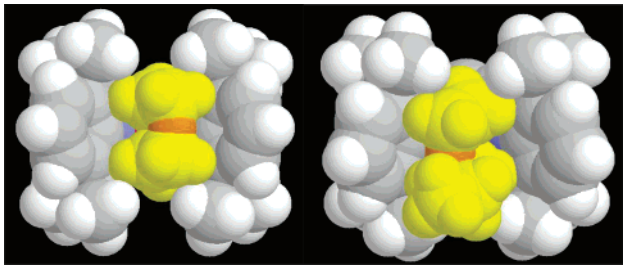

Figure 5. Space-filling representation for synchronous alkene exchange transition states (a) **5** and (b) **15**, both with Ar = 2,6-$^{i}Pr_2C_6H_3$ and R = Me, showing the ethene/ethyl and butene/butyl groups (both sets in yellow), with particular emphasis on the transferring hydrogen atom (orange).

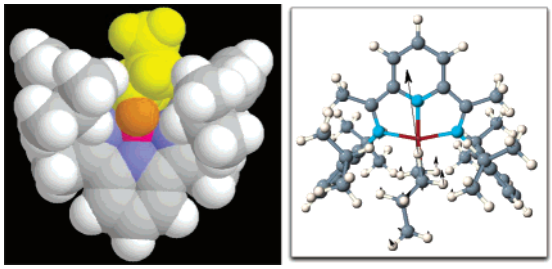

Figure 6. (a) Space-filling representation for the β-H transfer/elimination transition state **9** (Ar = 2,6-$^{i}Pr_2C_6H_3$, R = Me) and (b) ball-and-stick model of transition state **9**. The displacement vectors for the calculated imaginary normal mode (688i cm^{-1}) clearly identify it as a β-H elimination step.

ethenes) are 23.4 and 16.1 kcal mol^{-1} for Ar = R = H and Ar = 2,6-$^{i}Pr_2C_6H_3$, R = Me, respectively. Furthermore, a steric *acceleration* for the dissociative route of −7.3 kcal mol^{-1} is revealed, opposite of the steric *inhibition* anticipated for the associative mechanism. The transition state for the β-H transfer **3**, which precedes **1**, has barriers of 10.4 and 3.3 kcal mol^{-1} (Ar = R = H and Ar = 2,6-$^{i}Pr_2C_6H_3$, R = Me, respectively) relative to **6**, revealing a slightly smaller steric acceleration (of 6.3 kcal mol^{-1}). The homologous dissociative stepwise route with *n*-butyl replacing ethyl (**12** to **11**) has corresponding free energy barriers of 18.9 kcal mol^{-1} (Ar = R = H) and 9.0 kcal mol^{-1} (Ar = 2,6-$^{i}Pr_2C_6H_3$, R = Me), with a steric acceleration of −9.9 kcal mol^{-1}. The transition state **9** for β-H transfer on the dissociative pathway has a free energy barrier from **12** of 10.0 and 3.6 kcal mol^{-1}, respectively, again with a somewhat reduced steric acceleration (−6.4 kcal mol^{-1}) relative to ethyl/ethene exchange.

Alkene Exchange Equilibrium. The preceding arguments have established that the lowest energy mechanism for alkene exchange proceeds via transition state **9**, leading to a dissociative endpoint **11** (= **1** + butene), along with sterically induced lowering of the reaction barriers. It becomes convenient at this point to re-normalize the potential surface appropriate for considering the actually observed equilibrium:

$$\mathbf{8} + \text{ethene} = \mathbf{4} + \text{1-butene}$$

This is known experimentally to proceed from **8** to give **4**, and so we present the computed free energies summarizing these reactions in Scheme 7, normalized relative to species **8** + ethene (the left-hand side of the equilibrium). We have already noted that formation of the two alkene complexes **12** and **16** is actually inhibited by the sterically demanding ligand (Ar = 2,6-$^{i}Pr_2C_6H_3$, R = Me). The overall free energy of reaction is relatively unaffected by these steric effects, being −4.4 kcal mol^{-1} for Ar = R = H and −2.6 kcal mol^{-1} for Ar = 2,6-$^{i}Pr_2C_6H_3$, R = Me, and correctly favoring the right-hand side of the equilibrium.

Nature of the Transition State for Alkene Exchange. The remaining issues relate to the nature of the transition state for the alkene exchange mechanism. The conventional conclusion from the experimental observation of a kinetic isotope effect (k^H/k^D_{298} (d_9) = 3.3) for the exchange of d_9-**8** (d_9-**III**) with C_2D_4 is that the transition state must clearly involve C−H cleavage, and the temperature dependence of the reaction rate gives $\Delta G^{\ddagger}$ = 22.9 ± 0.9 kcal mol^{-1} and $\Delta S^{\ddagger}$ = +6 ± 3 cal mol^{-1} K^{-1}. These experimental values clearly exclude the synchronous route via **15** on the grounds of both the computed free energy barrier and its computed entropy ($\Delta S^{\ddagger}$ = −50.2 cal mol^{-1} K^{-1}). Of the two alternative species that might constitute the rate-limiting step, species **9** (Ar = 2,6-$^{i}Pr_2C_6H_3$, R = Me) has a small negative entropy ($\Delta S^{\ddagger}$ = −5.6 cal mol^{-1} K^{-1}) and directly involves C−H cleavage. This latter characteristic can be probed by calculating the value of k^H/k^D_{298} (d_9) using the Bigeleisen equations[16] and the rigid-rotor-harmonic-oscillator approximation. The value obtained of 3.8 is in reasonable agreement with the experimental value; its reduced value (from a normal value of around 7 for linear hydrogen transfers) is in accord with the nonlinearity of the Co−H−C transfer in **9**. The predicted free energy of activation ($\Delta G^{\ddagger}$ = 10.6 kcal mol^{-1}) is however significantly lower than measured, which raises doubts as to whether **9** is truly the structure of the rate-limiting species. Evidence that does support **9** is the substituent effect induced by replacing Ar = 2,6-$^{i}Pr_2C_6H_3$ by the sterically less demanding Ar = 2,4,6-$Me_3C_6H_2$. This experimentally is known to accelerate the rate of exchange with ethene by a factor of 16.3, which corresponds to a reduction in the free energy activation barrier of 1.6 kcal mol^{-1}. The calculated reduction of 2.5 kcal mol^{-1} tends to support this steric argument.

System **11**, which represents the dissociative endpoint and (total) energy maximum for the elimination of butene, is in better agreement with experiment than **9** in terms of overall free energy barrier ($\Delta G^{\ddagger}$ = 16.0 kcal mol^{-1}), but it deviates significantly in its predicted entropy of activation ($\Delta S^{\ddagger}$ = +52.0 cal mol^{-1} K^{-1}), which is nevertheless a value typical of a fully dissociative mechanism. Although no direct C−H cleavage is involved in **11**, the relatively large loss of zero-point energy as represented by the Co−H/D bond means that **11** also leads to a large predicted (in this case equilibrium) isotope effect of k^H/k^D_{298} = 5.4 (d_9). The isotope effect can be decomposed to k^H/k^D_{298} = 3.8 (d_1) when only the abstracted β-H is deuterated, and k^H/k^D_{298} = 1.4 (d_8) when the remainder of the *n*-butyl chain is deuterated. From this we conclude that the replacement of a C−H bond with a Co−H bond during this reaction will result in a large observed isotope effect regardless

(16) See: Maccoll, A. *Ann. Rep. Prog. Chem.* **1974**, *71*, 77−101.

of whether C−H cleavage is directly involved in the transition state. Observed isotope effects are therefore not necessarily an unambiguous indicator of the nature of the transition state.

The measurement of a small but positive entropy of activation implies that the kinetic transition state is looser in structure than **9**, but is more bound than the fully dissociated **11**. This is likely to be achieved somewhere in the potential region between species **10** and **11**. An optimized reaction path scan using the distance between the Co and the midpoint of the C=C bond of the butene as a reaction coordinate reveals there to be no obvious energy maximum other than the fully dissociated system **11**, and hence no defined transition state on this region of the total energy surface. This leads us to consider the possibility that this represents an example of a so-called barrierless reaction, in which the kinetics are determined by a transition state defined by the free energy and not the potential energy surface. Examples of such reactions are known, and a particularly relevant one relates to the reaction between substituted ethenes and a Cu catalyst.[17] No transition state in the potential energy surface was reported (at a level of theory similar to that used here), but approximate estimates of the free energy[17] suggested that the free energy surface does have a maximum higher than either reactant or product. Related observations have previously been made for the addition of carbenes to alkenes.[18] Such behavior for the reaction of **8** to **11** would imply a free energy barrier (marked with an asterisk (*) in Scheme 6) higher than that computed for **11**. This would reconcile the computed barrier by bringing it into closer agreement with experiment, and very probably both the entropy and the isotope effects would also match the experimental values.

Modeling Conclusions. We conclude that the computational modeling of this reaction has firmly established the following features: (a) modeling of the full system, i.e., including the bulky aryl substituents, is mechanistically essential. The steric effects arising from both the ketimine methyl (R) and the aryl (Ar) groups mediate the agostic interactions, inhibit associative pathways, accelerate dissociative routes, and play a vital role in one key transition state for β-H transfer; (b) calculating free energies clearly establishes that associative pathways are disfavored on entropic grounds; (c) pathways for C−C bond formation/alkene polymerization are clearly shown to be higher than those for alkene exchange, in accord with experiment; (d) hydrogen isotope effects for the alkene exchange mechanism are not necessarily diagnostic of an explicit C−H cleavage in the rate-determining step, but could also arise because of loss of zero-point energy in the formation of a Co−H bond; (e) no transition state characterized in the potential energy surface has the correct predicted combination of free energy barrier and entropy, and we conclude that the rate-limiting step is probably a barrierless reaction corresponding to a free energy maximum on the pathway for dissociation of butene from the complex **10**, which may have both a higher barrier than predicted for the formation of **11** alone and a much smaller entropy.

Overall Conclusions

A good agreement between experimental and computational studies was found in the description of β-hydrogen transfer in bis(imino)pyridine cobalt(I) *n*-alkyl complexes, particularly when entropic contributions were considered in the theoretical approach. Both studies independently conclude that alkene exchange occurs via a dissociative mechanism centered on a cobalt-hydride species. In view of this mutual overlap in the elucidation of alkene exchange, the mechanism may be considered to be reasonably well understood. Associative mechanisms for either alkene exchange or alkene insertion are evidently disfavored in the neutral cobalt(I) complexes considered.

Although the qualitative agreement between the experimental and computational findings is good, quantitative differences remain, which would probably be resolved in a more extensive theoretical scrutiny. The calculated kinetic and thermodynamic values for the relationship between LCo^{n}Bu (**III/8** with Ar = 2,6-^{i}Pr$_2$C$_6$H$_3$, R = Me) and LCoEt (**I/4**) of $\Delta G^{\ddagger} = 16.0$ kcal mol^{-1} (via **VIII/1**) and $\Delta G_{298} = -1.8$ kcal mol^{-1} fall somewhat short of the experimentally determined ones ($\Delta G^{\ddagger} = 22.9$ kcal mol^{-1} and ΔG_{298} about −3.5 to −4.0 kcal mol^{-1}). Despite the fact that the theoretical model provides a more refined understanding of the origins of isotope effect, there is some disagreement over the magnitude of the isotope effect (3.8−5.4 computed, 3.3 measured).

The fact that the stable species LCoH **1** (=**VIII**) represents the highest point on the calculated PES for dissociative mechanisms, with no kinetic stabilization from surrounding transition states, is possibly the most surprising result of the theoretical study. In view of other studies[17,18] it does not, however, appear unreasonable to postulate that **1** is probably surrounded by free energy barriers on either side for alkene association/dissociation, which were not located on the standard total energy surface. Further resolution of this issue must await the development of computational methodologies for the location and quantification of these kinetically stabilizing barriers and which are capable of handling systems of this size and complexity.

Experimental Methods

Computational Details. Calculations were performed using Gaussian 98 (revision A.11) and Gaussian 03 (revision B.04). Geometries were optimized at two levels. Exploratory studies were specified as B3LYP employing a 6-311G(d,p) basis set for Co and 6-31G(d,p) (Ar = R = H). The substituted systems (Ar = 2,6-^{i}Pr$_2$C$_6$H$_3$ or 2,4,6-Me$_3$C$_6$H$_2$, R = Me) were modeled at the same level, but using a STO-3G basis for the Ar and R = Me groups. Corrections for free energies were derived from a frequency calculation at these levels (including symmetry number corrections for ethene and species **1**). Transition states were characterized by the single negative root in the Hessian matrix exhibiting the appropriate normal mode. Coordinates and energies for computed species are available in the Supporting Information.

Experimental Details. With the exception of the ligand preparations, all reactions were carried out under an atmosphere of dry dinitrogen gas. Standard Schlenk-line and

(17) Rasmussen, T.; Jensen, J. F.; Østergaard, N.; Tanner, D.; Ziegler, T.; Norrby, P.-O. *Chem. Eur. J.* **2002**, *8*, 177.

(18) (a) Houk, K. N.; Rondan, N. G.; Mareda, J. *J. Am. Chem. Soc.* **1984**, *106*, 4291. (b) Houk, K. N.; Rondan, N. G. *J. Am. Chem. Soc.* **1984**, *106*, 4293.

associated techniques were employed for the manipulation of air-sensitive compounds. Conventional inert atmosphere dryboxes were used for the preparation of the analytical and spectroscopic samples, as well as for weighing and storage of air-sensitive compounds.

All starting materials were obtained from commercial sources. Ligands and cobalt(II) and cobalt(I) complexes were prepared as described previously.[1] With the exception of 1-butanol, pentane, and toluene, all solvents were dried by refluxing over an appropriate drying agent,[19] distilled, and degassed prior to use. Pentane, heptane, and toluene were dried according to a published procedure.[20] 1-Butanol was purchased in anhydrous grade and used as such. Pentane, heptane, toluene, and diethyl ether were stored over a K mirror, and THF was stored over molecular sieves.

All spectra were recorded at ambient temperature unless otherwise stated. All NMR spectra were recorded on a Bruker AC-250 (^{1}H and ^{13}C spectra at 250.133 and 62.896 MHz, respectively). On the occasions that higher field instruments were employed, spectra were recorded on either a Bruker DRX-400 (^{1}H and ^{13}C spectra at 400.129 and 100.613 MHz, respectively) or a Bruker AM-500 (^{1}H resonance at 500.133 MHz). ^{1}H and ^{13}C spectra were referenced internally (the former to the residual protium signal of the deuterated solvents, the latter directly to the ^{13}C multiplets due the resonance signals of the NMR solvent) and are reported relative to the chemical shift of tetramethylsilane.

Preparation of Complexes. Preparation of [Co(CH$_2$CH$_3$){N$_3$(dipp)$_2$}], I. The precursor complex [CoCl$_2$-{N$_3$(dipp)$_2$}] (306 mg, 0.500 mmol) was treated with ethylmagnesium chloride (0.50 cm^3 of a 3.0 M solution in Et$_2$O, 1.50 mmol) in diethyl ether (20 cm^3) at −78 °C and allowed to warm to 0 °C over 24 h, followed by removal of all volatiles under reduced pressure. Extraction with pentane (30 cm^3), followed by filtration and solvent removal from the supernatant, afforded an intensely colored solid that was dried in vacuo at 30 °C for 30 min. Isolated yield: typically 120−150 mg, 42−53% based on [CoCl$_2${N$_3$(dipp)$_2$}].

^{1}H NMR (C$_6$D$_6$): δ 10.25 (1H, t, $^3J_{H-H}$ = 7.6 Hz; *p-H*, py), 7.99 (2H, d, $^3J_{H-H}$ = 7.6 Hz; *m-H*, py), 7.51 (2H, distorted triplet, $^3J_{H-H}$ = 7.7 Hz; *p-H*, Ar), 7.39 (4H, distorted doublet, $^3J_{H-H}$ = 7.7 Hz; *m-H*, Ar), 3.14 (4H, septet, $^3J_{H-H}$ = 6.8 Hz; (CH$_3$)C*H*(CH$_3$)), 1.51 (2H, q, $^3J_{H-H}$ = 7.9 Hz; CoC*H*$_2$CH$_3$), 1.17 (12H, d, $^3J_{H-H}$ = 6.8 Hz; (C*H*$_3$)CH(CH$_3$)), 0.74 (12H, d, $^3J_{H-H}$ = 6.8 Hz; (CH$_3$)CH(C*H*$_3$)), −1.18 (3H, t, $^3J_{H-H}$ = 7.9 Hz; CoCH$_2$C*H*$_3$; $^1J_{H-C}$ = 123 Hz), −1.33 (6H, s; ArN=CC*H*$_3$). ^{13}C{^{1}H} NMR δ (C$_6$D$_6$): 165.2 (ArN=*C*CH$_3$), 157.8 (*o-C*, py), 154.9 (*i-C*, Ar), 140.8 (*o-C*, Ar), 126.6 (*p-C*, Ar), 124.1 (*m-C*, Ar), 122.6 (*m-C*, py), 117.6 (*p-C*, py), 28.5 ((CH$_3$)*C*H(CH$_3$)), 26.4 (ArN=C*C*H$_3$), 24.3 ((*C*H$_3$)CH(CH$_3$)), 23.3 ((CH$_3$)CH(*C*H$_3$)), 13.0 (CoCH$_2$*C*H$_3$), −0.5 (Co*C*H$_2$CH$_3$).

Preparation of [Co(CH$_2$CH$_2$CH$_3$){N$_3$(dipp)$_2$}], II. Using a procedure similar to that employed for **I**, the title compound was isolated in yields of 120−150 mg (41−51%) from 0.500 mmol of [CoCl$_2${N$_3$(dipp)$_2$}] (306 mg) and 1.50 mmol of *n*-propylmagnesium chloride (0.75 cm^3 of a 2.0 M solution in Et$_2$O.

^{1}H NMR (C$_6$D$_6$): δ 10.25 (1H, t, $^3J_{H-H}$ = 7.6 Hz; *p-H*, py), 7.98 (2H, d, $^3J_{H-H}$ = 7.6 Hz; *m-H*, py), 7.52 (2H, distorted triplet, $^3J_{H-H}$ = 7.8 Hz; *p-H*, Ar), 7.40 (4H, distorted doublet, $^3J_{H-H}$ = 7.8 Hz; *m-H*, Ar), 3.12 (4H, septet, $^3J_{H-H}$ = 6.8 Hz; (CH$_3$)C*H*(CH$_3$)), 1.31 (2H, m; Co*C*H$_2$CH$_2$CH$_3$; $^1J_{H-C}$ = 119 Hz), 1.17 (12H, d, $^3J_{H-H}$ = 6.8 Hz; (C*H*$_3$)CH(CH$_3$)), 0.78 (12H, d, $^3J_{H-H}$ = 6.8 Hz; (CH$_3$)CH(C*H*$_3$)), 0.50 (3H, t, $^3J_{H-H}$ = 7.1 Hz; CoCH$_2$CH$_2$C*H*$_3$; $^1J_{H-C}$ = 123 Hz), −0.73 (2H, m; CoCH$_2$C*H*$_2$CH$_3$; $^1J_{H-C}$ = 125 Hz), −1.31 (6H, s; ArN=CC*H*$_3$). ^{13}C{^{1}H} NMR (C$_6$D$_6$): δ 165.3 (ArN=*C*CH$_3$), 157.7 (*o-C*, py), 155.1 (*i-C*, Ar), 140.8 (*o-C*, Ar), 126.5 (*p-C*, Ar), 124.0 (*m-C*, Ar), 122.6 (*m-C*, py), 117.6 (*p-C*, py), 28.5 ((CH$_3$)*C*H(CH$_3$)), 26.4 (ArN=C*C*H$_3$), 24.4 ((*C*H$_3$)CH(CH$_3$)), 23.4 ((CH$_3$)CH(*C*H$_3$)), 21.8 (CoCH$_2$*C*H$_2$CH$_3$), 16.2 (CoCH$_2$CH$_2$*C*H$_3$), 1.5 (Co*C*H$_2$CH$_2$CH$_3$). EI-MS (*m/z*): 539 [Co{N$_3$(dipp)$_2$}], 82%; 466, 46%; 308, 78%; 90, 100%.

Preparation of [Co(CH$_2$CH$_2$CH$_2$CH$_3$){N$_3$(dipp)$_2$}], III. Using a procedure similar to that employed for **I**, the title compound was isolated in yields of 120−150 mg (40−50%) from 0.500 mmol of [CoCl$_2${N$_3$(dipp)$_2$}] (306 mg) and 1.50 mmol of *n*-butylmagnesium chloride (0.75 cm^3 of a 2.0 M solution in Et$_2$O).

^{1}H NMR (C$_6$D$_6$): δ 10.24 (1H, t, $^3J_{H-H}$ = 7.6 Hz; *p-H*, py), 7.99 (2H, d, $^3J_{H-H}$ = 7.6 Hz; *m-H*, py), 7.52 (2H, distorted triplet, $^3J_{H-H}$ = 7.7 Hz; *p-H*, Ar), 7.40 (4H, distorted doublet, $^3J_{H-H}$ = 7.7 Hz; *m-H*, Ar), 3.11 (4H, septet, $^3J_{H-H}$ = 6.8 Hz; (CH$_3$)C*H*(CH$_3$)), 1.28 (2H, m; Co*C*H$_2$CH$_2$CH$_2$CH$_3$), 1.17 (12H, d, $^3J_{H-H}$ = 6.8 Hz; (C*H*$_3$)CH(CH$_3$)), 0.87 (2H, m; CoCH$_2$CH$_2$C*H*$_2$-CH$_3$), 0.79 (12H, d, $^3J_{H-H}$ = 6.8 Hz; (CH$_3$)CH(C*H*$_3$)), 0.61 (3H, t, $^3J_{H-H}$ = 7.3 Hz; CoCH$_2$CH$_2$CH$_2$C*H*$_3$), −0.85 (2H, m; CoCH$_2$C*H*$_2$CH$_2$CH$_3$), −1.31 (6H, s; ArN=CC*H*$_3$). ^{13}C{^{1}H} NMR (C$_6$D$_6$): δ 165.2 (ArN=*C*CH$_3$), 157.7 (*o-C*, py), 155.0 (*i-C*, Ar), 140.9 (*o-C*, Ar), 126.4 (*p-C*, Ar), 124.0 (*m-C*, Ar), 122.6 (*m-C*, py), 117.6 (*p-C*, py), 30.5 (CoCH$_2$*C*H$_2$CH$_2$CH$_3$), 28.5 ((CH$_3$)*C*H-(CH$_3$)), 26.4 (ArN=C*C*H$_3$), 24.5 ((*C*H$_3$)CH(CH$_3$)), 23.4 ((CH$_3$)-CH(*C*H$_3$)), 14.2 (CoCH$_2$CH$_2$*C*H$_2$CH$_3$), 13.7 (CoCH$_2$CH$_2$CH$_2$*C*H$_3$), −2.2 (Co*C*H$_2$CH$_2$CH$_2$CH$_3$).

Preparation of [Co(CH$_2$CH$_2$CH$_2$CH$_2$CH$_2$CH$_3$)-{N$_3$(dipp)$_2$}], IV. Using a procedure similar to that employed for **I**, the title compound was isolated in yields of 150−190 mg (48−61%) from 0.500 mmol of [CoCl$_2${N$_3$(dipp)$_2$}] (306 mg) and 1.50 mmol of *n*-hexylmagnesium bromide (0.75 cm^3 of a 2.0 M solution in Et$_2$O).

^{1}H NMR (C$_6$D$_6$): δ 10.23 (1H, t, $^3J_{H-H}$ = 7.6 Hz; *p-H*, py), 8.00 (2H, d, $^3J_{H-H}$ = 7.6 Hz; *m-H*, py), 7.52 (2H, distorted triplet, $^3J_{H-H}$ = 7.7 Hz; *p-H*, Ar), 7.40 (4H, distorted doublet $^3J_{H-H}$ = 7.7 Hz; *m-H*, Ar), 3.11 (4H, septet, $^3J_{H-H}$ = 6.8 Hz; (CH$_3$)C*H*(CH$_3$)), 1.28 (2H, m; Co*C*H$_2$CH$_2$CH$_2$CH$_2$CH$_2$CH$_3$), 1.17 (12H, d, $^3J_{H-H}$ = 6.8 Hz; (C*H*$_3$)CH(CH$_3$)), 1.04 (2H, m; CoCH$_2$CH$_2$CH$_2$CH$_2$C *H*$_2$CH$_3$), 0.96 (2H, m; CoCH$_2$CH$_2$CH$_2$-C*H*$_2$CH$_2$CH$_3$), 0.83 (∼2H, multiplet partially overlapping with triplet from Co(CH$_2$)$_5$C*H*$_3$; CoCH$_2$CH$_2$C*H*$_2$CH$_2$CH $_2$CH$_3$), 0.81 (∼3H, triplet partially overlapping with doublet from (CH$_3$)-CH(C*H*$_3$), $^3J_{H-H}$ = 7.0 Hz; Co(CH$_2$)$_5$C*H*$_3$), 0.79 (∼12H, d, $^3J_{H-H}$ = 6.8 Hz; (CH$_3$)CH(C*H*$_3$)), −0.83 (2H, m; CoCH$_2$C*H*$_2$CH$_2$CH$_2$-CH$_2$CH$_3$), −1.31 (6H, s; ArN=CC*H*$_3$). ^{13}C{^{1}H} NMR (C$_6$D$_6$): 165.2 (ArN=*C*CH$_3$), 157.7 (*o-C*, py), 155.0 (*i-C*, Ar), 140.9 (*o-C*, Ar), 126.5 (*p-C*, Ar), 124.0 (*m-C*, Ar), 122.5 (*m-C*, py), 117.6 (*p-C*, py), 31.9 (CoCH$_2$CH$_2$*C*H$_2$CH$_2$CH$_2$CH$_3$), 31.5 (CoCH$_2$CH$_2$-CH$_2$*C*H$_2$CH $_2$CH$_3$), 28.5 ((CH$_3$)*C*H(CH$_3$)), 27.9 (CoCH$_2$*C*H$_2$CH$_2$-CH$_2$CH $_2$CH$_3$), 26.4 (ArN=C*C*H$_3$), 24.5 ((*C*H$_3$)CH(CH$_3$)), 23.4 ((CH$_3$)CH(*C*H$_3$)), 22.9 (CoCH$_2$CH$_2$CH$_2$CH$_2$ *C*H$_2$CH$_3$), 14.5 (Co(CH$_2$)$_5$*C*H$_3$), −1.7 (Co*C*H$_2$CH$_2$CH$_2$CH$_2$CH$_2$CH $_2$CH$_3$).

Preparation of [Co(CH$_2$CH$_2$Ph){N$_3$(dipp)$_2$}], V. The synthesis was very similar to that of **I**, as described above. [CoCl$_2${N$_3$(dipp)$_2$}] (489 mg, 0.750 mmol) was treated with 2-phenylethylmagnesium chloride (2.25 cm^3 of a 1.0 M solution in THF, 2.25 mmol) in diethyl ether (30 cm^3) at −78 °C, allowed to warm to 0 °C over 24 h, and subsequently stirred for half an hour at ambient temperature, followed by removal of all volatiles under reduced pressure. Extraction with a mixture of pentane (30 cm^3) and toluene (15 cm^3), filtration, and solvent removal from the supernatant afforded a solid, which was dried in vacuo at 30 °C for 30 min. Isolated yield: typically 180−240 mg, 37−50% based on [CoCl$_2${N$_3$(dipp)$_2$}].

^{1}H NMR (C$_6$D$_6$): δ 10.21 (1H, t, $^3J_{H-H}$ = 7.6 Hz; *p-H*, py), 7.90 (2H, d, $^3J_{H-H}$ = 7.6 Hz; *m-H*, py), 7.60 (2H, distorted triplet, $^3J_{H-H}$ = 7.8 Hz; *p-H*, Ar), 7.45 (4H, distorted doublet, $^3J_{H-H}$ = 7.8 Hz; *m-H*, Ar), 7.11 (2H, m; *m-H*, CoCH$_2$CH$_2$*Ph*),

(19) Armarego, W. L. F.; Perrin, D. D. *Purification of Laboratory Chemicals*, 4th ed.; Butterworth/Heinemann: Oxford, 1998.
(20) Pangborn, A. B.; Giardello, M. A.; Grubbs, R. H.; Rosen, R. K.; Timmers, F. J. *Organometallics* **1996**, *15*, 1518.

6.92 (1H, broadened triplet, $^3J_{H-H}$ ca. 7.3 Hz; *p-H*, $CoCH_2CH_2Ph$), 6.61 (2H, broadened doublet, $^3J_{H-H}$ ca. 7.1 Hz; *o-H*, $CoCH_2CH_2Ph$), 3.11 (4H, septet, $^3J_{H-H}$ = 6.8 Hz; $(CH_3)CH(CH_3)$), 1.19 (~2H, multiplet partially overlapping with doublet from $(CH_3)CH(CH_3)$; $CoCH_2CH_2Ph$), 1.17 (~12H, d, $^3J_{H-H}$ = 6.8 Hz; $(CH_3)CH(CH_3)$), 0.72 (12H, d, $^3J_{H-H}$ = 6.8 Hz; $(CH_3)CH(CH_3)$), 0.32 (2H, m; $CoCH_2CH_2Ph$), −1.22 (6H, s; ArN=CCH_3). $^{13}C\{^1H\}$ NMR (C_6D_6): δ 165.6 (ArN=*C*CH_3), 157.1 (*o-C*, py), 154.9 (*i-C*, Ar), 147.6 (*i-C*, $CoCH_2CH_2Ph$), 141.2 (*o-C*, Ar), 128.1 (*o-C*, $CoCH_2CH_2Ph$), 127.9 (*m-C*, $CoCH_2CH_2Ph$), 126.6 (*p-C*, Ar), 124.3 (*m-C*, Ar), 124.1 (*p-C*, $CoCH_2CH_2Ph$), 122.8 (*m-C*, py), 117.6 (*p-C*, py), 36.7 ($CoCH_2CH_2Ph$), 28.6 ($(CH_3)CH(CH_3)$), 26.2 (ArN=CCH_3), 24.5 ($(CH_3)CH(CH_3)$), 23.5 ($(CH_3)CH(CH_3)$), 1.2 ($CoCH_2CH_2Ph$).

Preparation of [Co(CH$_2$CH$_3$){N$_3$(mes)$_2$}], VI. Addition of ethylmagnesium chloride (0.50 cm^3 of a 3.0 M solution in Et_2O, 1.50 mmol) to a suspension of $[CoCl_2\{N_3(mes)_2\}]$ (264 mg, 0.500 mmol) in diethyl ether (40 cm^3) at −78 °C gave a mixture, which was allowed to warm to 0 °C over 24 h, followed by removal of all volatiles under reduced pressure. Extraction with toluene (50 cm^3), followed by filtration and solvent removal from the supernatant, afforded an intensely colored solid that was dried in vacuo at 25−30 °C for 30 min. Isolated yield: 125 mg, 51% based on $[CoCl_2\{N_3(mes)_2\}]$.

Alternatively, this compound may be prepared in situ by reaction of **VII** with a small excess of ethylene in C_6D_6. Yield quantitative by ^1H NMR.

^1H NMR (C_6D_6): δ 10.18 (1H, t, $^3J_{H-H}$ = 7.6 Hz; *p-H*, py), 8.07 (2H, d, $^3J_{H-H}$ = 7.6 Hz; *m-H*, py), 7.06 (4H, s; *m-H*, Ar), 2.30 (6H, s; *p*-CH3, Ar), 2.04 (12H, s; *o*-CH3, Ar), 1.31 (2H, q, $^3J_{H-H}$ = 8.0 Hz; $CoCH_2CH_3$), −1.33 (3H, t, $^3J_{H-H}$ = 8.0 Hz; $CoCH_2CH_3$), −1.48 (6H, s; ArN=CCH_3). $^{13}C\{^1H\}$ NMR (C_6D_6): δ 164.3 (ArN=*C*CH_3), 158.3 (*o-C*, py), 155.1 (*i-C*, Ar), 134.4 (*p-C*, Ar), 129.7 (*o-C*, Ar), 129.5 (*m-C*, Ar), 121.6 (*m-C*, py), 117.9 (*p-C*, py), 24.9 (ArN=C*C*H_3), 21.3 (*p-C*H_3, Ar), 19.1 (*o-C*H_3, Ar), 10.8 ($CoCH_2CH_3$), −11.5 ($CoCH_2CH_3$).

Preparation of [Co(CH$_2$CH$_2$CH$_2$CH$_3$){N$_3$(mes)$_2$}], VII. Using a procedure similar to that employed for **I**, the title compound was isolated in yields of 120−150 mg (fw = 513.6) (47−58%) from 0.500 mmol of $[CoCl_2\{N_3(mes)_2\}]$ (264 mg) and 1.50 mmol of *n*-butylmagnesium chloride (0.75 cm^3 of a 2.0 M solution in Et_2O).

^1H NMR (C_6D_6): δ 10.25 (1H, t, $^3J_{H-H}$ = 7.6 Hz; *p-H*, py), 8.05 (2H, d, $^3J_{H-H}$ = 7.6 Hz; *m-H*, py), 7.08 (4H, s; *m-H*, Ar), 2.33 (6H, s; *p*-CH_3, Ar), 2.04 (12H, s; *o*-CH_3, Ar), 1.18 (2H, m; $CoCH_2CH_2CH_2CH_3$), 0.71 (2H, m; $CoCH_2CH_2CH_2CH_3$), 0.58 (3H, t, $^3J_{H-H}$ = 7.2 Hz; $CoCH_2CH_2CH_2CH_3$), −1.16 (2H, m; $CoCH_2CH_2CH_2CH_3$), −1.53 (6H, s; ArN=CCH_3). $^{13}C\{^1H\}$ NMR (C_6D_6): δ 164.6 (ArN=*C*CH_3), 158.4 (*o-C*, py), 155.4 (*i-C*, Ar), 134.4 (*p-C*, Ar), 129.7 (*o-C*, Ar), 129.4 (*m-C*, Ar), 121.7 (*m-C*, py), 117.9 (*p-C*, py), 28.5 ($CoCH_2CH_2CH_2CH_3$), 25.4 ($CoCH_2CH_2CH_2CH_3$), 25.1 (ArN=C*C*H_3), 21.3 (*p-C*H_3, Ar), 19.2 (*o-C*H_3, Ar), 13.6 ($CoCH_2CH_2CH_2CH_3$), −3.3 ($CoCH_2CH_2CH_2CH_3$).

NMR-Scale Reactions. Reaction of [Co(CH$_2$CH$_2$R)-{N$_3$(Ar)$_2$}] (II−V, VII) with a 1-Alkene. In an NMR tube, a solution of $[Co(CH_2CH_2R)\{N_3(Ar)_2\}]$ (**II**−**V**, **VII**) (typically 0.030 mmol) in 0.6−0.7 cm^3 C_6D_6 was degassed by two freeze−pump−thaw cycles and frozen again, and the tube was evacuated. Subsequently, the desired quantity of 1-alkene gas was condensed (77 K) onto the frozen solution. The solution was thawed and shaken just prior to examination by NMR. Data characterizing $[Co(CH_2CH_3)\{N_3(Ar)_2\}]$ (**I**, **VI**), and $[Co(CH_2CH_2R)\{N_3(Ar)_2\}]$ (**II**−**V**, **VII**) are as given previously. The liquid 1-alkene 1-hexene was simply added to the solution if and when required.

Preparation of [CoH{N$_3$(dipp)$_2$}], VIII. A solution of $[CoMe\{N_3(dipp)_2\}]$ (5.6 mg, 0.010 mmol) in C_6D_6 (0.7 cm^3) was degassed by two freeze−pump−thaw cycles. A stoichiometric quantity of room-temperature hydrogen gas was then rapidly admitted into the vacuum above the solution, frozen at 77 K. The solution was allowed to thaw and mixed with the gas by repeated shaking. Other cobalt(I) *n*-alkyl reagents may be used as reaction precursors in place of $[CoMe\{N_3(dipp)_2\}]$. Yield: >98% by NMR; only byproduct (<2%) is uncomplexed ligand. The volatiles may be trapped into another NMR tube for further characterization.

^1H NMR (C_6D_6): δ 10.83 (1H, t, $^3J_{H-H}$ = 7.6 Hz; *p-H*, py), 7.60 (2H, distorted triplet, $^3J_{H-H}$ = 7.7 Hz; *p-H*, Ar), 7.59 (2H, d, $^3J_{H-H}$ = 7.6 Hz; *m-H*, py), 7.46 (4H, distorted doublet, $^3J_{H-H}$ = 7.7 Hz; *m-H*, Ar), 3.42 (4H, septet, $^3J_{H-H}$ = 6.8 Hz; $(CH_3)CH(CH_3)$), 1.31 (12H, d, $^3J_{H-H}$ = 6.8 Hz; $(CH_3)CH(CH_3)$), 0.28 (12H, d, $^3J_{H-H}$ = 6.8 Hz; $(CH_3)CH(CH_3)$), −1.66 (6H, s; ArN=CCH_3). No resonance for Co−H is detected within +100 to −150 [$I(^{59}Co)$ = 7/2]. $^{13}C\{^1H\}$ NMR (C_6D_6): δ 168.6 (ArN=*C*CH_3), 160.1 (*i-C*, Ar), 156.5 (*o-C*, py), 140.2 (*o-C*, Ar), 126.3 (*p-C*, Ar), 124.2 (*m-C*, Ar), 123.7 (*m-C*, py), 118.0 (*p-C*, py), 28.9 ($(CH_3)CH(CH_3)$), 25.6 (ArN=C*C*H_3), 23.6 ($(CH_3)CH(CH_3)$), 22.7 ($(CH_3)CH(CH_3)$).

Reaction of [CoH{N$_3$(dipp)$_2$}] VIII with 1-Alkenes (C$_2$H$_4$, C$_3$H$_6$, 1-C$_4$H$_8$). A solution of $[CoH\{N_3(dipp)_2\}]$ **VIII** (0.010 mmol prepared in situ) in C_6D_6 (0.65 cm^3) was degassed by two freeze−pump−thaw cycles, frozen again, and evacuated. Subsequently, the desired quantity of 1-alkene (V = 5.0 cm^3, p = 220 mbar; n = 0.045 mmol) was condensed onto the solution. The solution was thawed and gently shaken just prior to examination by NMR. The principal reaction product (>80%), either **I**, **II**, or **III**, was characterized by ^1H and $^{13}C\{^1H\}$ NMR (spectroscopic details given above).

Attempted Preparation of [CoD{N$_3$(dipp)$_2$}], *d*$_1$-VIII. Attempted synthesis was analogous to that of VIII. A degassed solution of $[CoMe\{N_3(dipp)_2\}]$ (8.9 mg, 0.016 mmol) in C_6D_6 (0.7 cm^3) was frozen (77 K), and an excess (3.5 equiv) of room-temperature deuterium gas ($^2H_2$) was rapidly expanded into the vacuum above the frozen solution. The solution was subsequently allowed to thaw and mixed with the gas by repeated shaking. Yield: 80−90% by NMR (about 10%−20% uncomplexed ligand).

The resonance signals of the ^{i}Pr group ($\delta(^1H)$ = 3.42, 1.31, 0.28 ppm) are broadened and of diminished area (methine = 3.8/4.0H, sum of methyls = 16.0/24.0H), the total reduction in integral size correlating with the quantity of employed deuterium gas. In the ^{13}C NMR, a complex arrangement of overlapping but slightly shifted multiplets ($\Delta\delta$ around a few tenths of a ppm) is seen in the region of the ^{i}Pr group's signals. The observed coupling patterns are indicative of extensive, nonselective deuteration ($I(^2H)$ = 1) in all three chemical shift environments. All other resonance signals are as given for **VIII**, above.

Hydrolysis of the reaction product with methanol and dilute hydrochloric acid, followed by extraction with CH_2Cl_2 and removal of solvent from the organic layer, afforded uncomplexed ligand. Analysis of the free ligand by mass spectroscopy confirmed multiple deuteration of the ligand framework. Attempts to rapidly trap LCoD with an alkene always afforded bis(imino)pyridine cobalt complexes bearing nonlabeled *n*-alkyl chains, but containing partially deuterated ligand.

Acknowledgment. The authors wish to thank BP Chemicals Ltd. for funding.

Supporting Information Available: ^1H NMR spectra and NOE data for **I**−**VII**, coordinates (Molfile) and energies for computed species **1**−**16**, details of KIE calculations. This material is available free of charge via the Internet at http://pubs.acs.org.

OM049581H